



HAL
open science

Pressure-Dependent Photoluminescence Study of Wurtzite InP Nanowires

Nicolas Chauvin, Amaury Mavel, G. Patriarche, Bruno Masenelli, Michel Gendry, D. Machon

► **To cite this version:**

Nicolas Chauvin, Amaury Mavel, G. Patriarche, Bruno Masenelli, Michel Gendry, et al.. Pressure-Dependent Photoluminescence Study of Wurtzite InP Nanowires. *Nano Letters*, 2016, 16 (5), pp.2926-2930. 10.1021/acs.nanolett.5b04646 . hal-01489142

HAL Id: hal-01489142

<https://hal.science/hal-01489142>

Submitted on 3 May 2023

HAL is a multi-disciplinary open access archive for the deposit and dissemination of scientific research documents, whether they are published or not. The documents may come from teaching and research institutions in France or abroad, or from public or private research centers.

L'archive ouverte pluridisciplinaire **HAL**, est destinée au dépôt et à la diffusion de documents scientifiques de niveau recherche, publiés ou non, émanant des établissements d'enseignement et de recherche français ou étrangers, des laboratoires publics ou privés.

Pressure dependent photoluminescence study of wurtzite InP nanowires

Nicolas Chauvin¹, Amaury Mavel^{1,2}, Gilles Patriarche³, Bruno Masenelli¹, Michel Gendry², Denis Machon⁴.

¹ Université de Lyon, Institut des Nanotechnologies de Lyon (INL)-UMR5270-CNRS,

INSA-Lyon, 7 avenue Jean Capelle, 69621 Villeurbanne, France.

² Université de Lyon, Institut des Nanotechnologies de Lyon (INL)-UMR5270-CNRS,

Ecole Centrale de Lyon, 36 avenue Guy de Collongue, 69134 Ecully, France

³ Laboratoire de Photonique et de Nanostructures (LPN), CNRS, Université Paris-Saclay, route de Nozay, F-91460 Marcoussis, France.

⁴ Institut Lumière Matière, UMR 5306 Université Lyon 1-CNRS, Université de Lyon 69622 Villeurbanne cedex, France

KEYWORDS: InP nanowires, wurtzite material, high-pressure, optical properties, deformation potentials.

ABSTRACT .

The elastic properties of InP nanowires are investigated by photoluminescence measurements under hydrostatic pressure at room temperature and experimentally deduced values of the linear pressure coefficients are obtained. The pressure-induced energy shift of the A and B transitions yields a linear pressure coefficient of $\alpha_A = 88.2 \pm 0.5$ meV/GPa and $\alpha_B = 89.3 \pm 0.5$ meV/GPa with a small sublinear term of $\beta_A = \beta_B = -2.7 \pm 0.2$ meV/GPa². Effective hydrostatic deformation potentials of -6.12 ± 0.04 eV and -6.2 ± 0.04 eV are derived from the results for the A and B transitions, respectively. A decrease of the integrated intensity is observed above 0.5 GPa and is interpreted as a carrier transfer from the first to the second conduction band of the wurtzite InP.

INTRODUCTION

The integration of InP based nanowires (NWs) on silicon has attracted an intense interest to merge efficient optoelectronic devices with silicon (Si) based electronics. The monolithic growth of InP NWs on Si or InP substrates has already been investigated to design highly efficient solar cells,¹ lasers² or light emitted diodes.³ InP NWs grown on Si substrates present usually a wurtzite (Wz) crystallographic phase. Contrary to III-Nitrides semiconductors, there is no Wz substrate for III-V semiconductors such as InP, InAs or GaAs. As a consequence, the investigation of the optical, structural, mechanical or electronic properties of these Wz materials requires working directly on the NW geometry. This situation has a direct implication on the knowledge of these Wz semiconductor band parameters. There is a lack of experimental values for parameters such as the elastic coefficients, deformation potentials, piezoelectric coefficients or effective masses and it is necessary to rely on theoretical values.^{4,5} As far as the deformation potentials of Wz InP are concerned, only one theoretical paper has been published on this issue.⁶ Three different sets of parameters have been proposed based on three different *ab initio* approaches. High-pressure studies of semiconductor materials can give access to the hydrostatic deformation potentials and to the linear pressure coefficients.⁷ The interest for investigating III-V materials with a Wz crystallographic phase is reinforced by a specificity of the wurtzite band structure. Since the Wz structure has four atoms per cell while the zinc-blende (ZB) structure has only two atoms, there are twice more as many bands per k points in the Wz one. As a consequence, the Wz band structure contains two conduction bands: one associated with a direct emission and a second one with a pseudo-direct one.^{8,9} In the case of GaAs and InP Wz materials, the energy spacing between these two bands is expected to be relatively small: in the order of 30 meV for GaAs⁹ and between 0.2 to

0.4 eV for InP.^{10,4} As shown by *Signorello et al*,⁹ the small energy spacing in Wz GaAs NWs can be tuned using an uniaxial stress to control the optical and/or electrical properties of the material.

In this paper, the optical properties of Wz InP NWs have been investigated by high pressure photoluminescence at room temperature. These measurements allow us to extract the linear and quadratic pressure coefficients as well as the effective hydrostatic deformation potentials.

EXPERIMENTAL DETAILS

The Wz InP NW sample was grown on a Si(111) substrate by VLS-ssMBE using Au-In droplets as catalyst *in-situ* deposited at 500°C. Two growth steps were performed at different substrate temperatures to obtain the NWs. First, the NWs were grown during 10 minutes at 380°C with a indium beam equivalent pressure (BEP) corresponding to an InP 2D layer equivalent growth rate of 1 ML/s and with a P_V/P_{III} BEP ratio equal to 20 in order to produce pure Wz InP NWs.^{11,12} To increase the NW diameter, a second growth step of 20 minutes was performed at a lower temperature (340°C) to favor the NW radial growth.

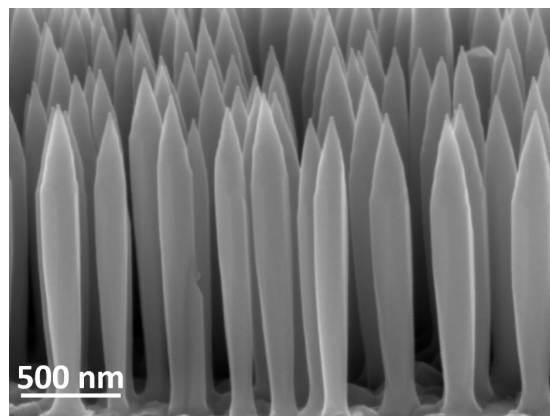


Figure 1: SEM picture of the InP NWs on Si substrate.

Scanning electron microscopy (SEM) studies revealed an averaged 1.7 μm length for these NWs (Figure 1). As far as the diameter is concerned a variation is observed as a function of the distance from the surface leading first to an inverse tapered geometry. An average diameter of 120 nm is observed at the NW foot while an average diameter of 190 nm is measured at 1.1-1.3 μm from the surface. Then the NWs present a tapering for the last 400-600 nm. TEM studies have been performed on the NWs (see supplementary material). The NWs have a perfect Wz crystallographic phase during the first 0.9-1 μm length. This length corresponds to the typical size of the InP NWs after the initial 10 min axial growth at 380°C. Then, some ZB insertions are observed in the upper part of the NWs. This part is related to the axial growth of the NWs during the 20 min growth at 340°C.¹² This second step is required to favor radial growth to increase the NW diameter: the NWs have usually a diameter in the 50-60 nm range after the first growth step. After the second step, the NW diameter is at least 10 times bigger than the exciton Bohr radius of Wz InP which means that no quantum confinement is expected.¹³ As far as the elastic coefficients are concerned, the Young modulus of these InP NWs should be similar to the bulk value.¹⁴ From these theoretical and experimental results we assume that our InP NWs can be considered as bulk material.

The high pressure photoluminescence measurements were carried out using a diamond anvil cell with low-fluorescence diamonds having a culet size of 350 μm . The NWs were mechanically removed from the growth substrate and loaded into a hole drilled in a stainless steel gasket. To obtain a hydrostatic pressure, a standard 4:1 methanol-ethanol mixture was used as the pressure transmitting medium. The optical properties of the Wz InP NWs were investigated by photoluminescence (PL) measurements performed using a 50 mW 532 nm continuous wave (cw)

diode-pumped solid-state laser as the excitation source and a nitrogen cooled silicon CCD detector coupled to a monochromator for the detection.

RESULTS AND DISCUSSIONS

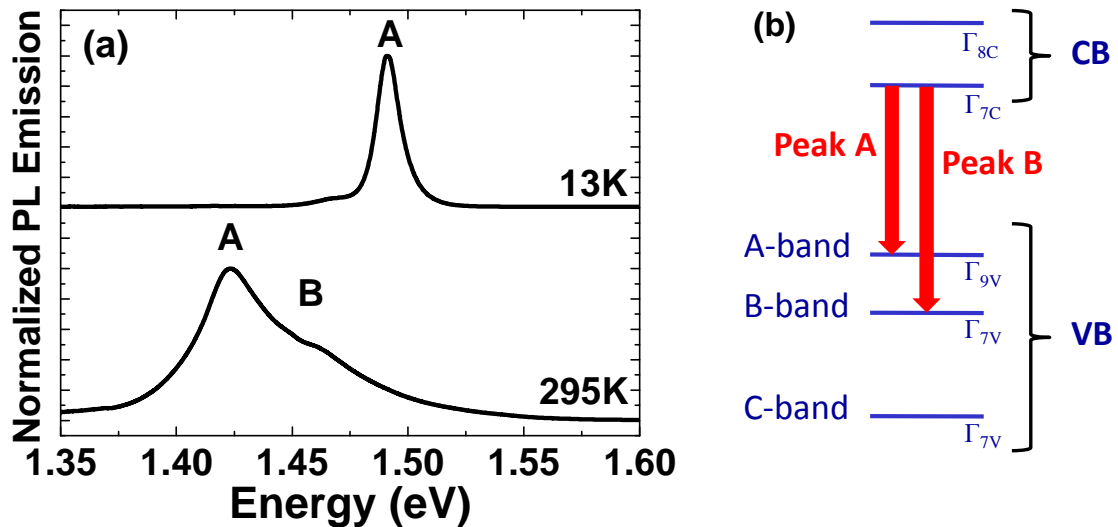
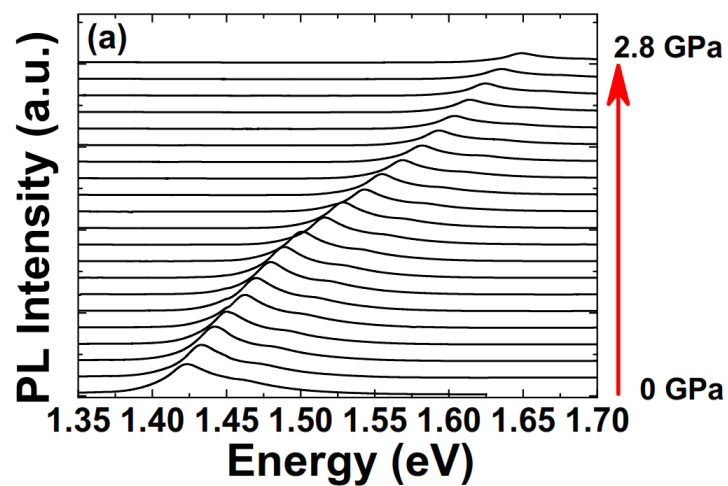


Figure 2: (a) PL emission from the InP NWs measured at 13K and 295K. (b) Schematic of the band energies at the Γ point in Wz InP.

Figure 2.a shows the PL emission from the InP NWs recorded at 13K and at room temperature. To understand the band structure of Wz NWs, spin-orbit coupling and crystal field splitting must be considered. These interactions split the valence band (VB) of the Wz crystal into a heavy-hole (usually labeled A-band), a light-hole (B-band) and a split-off band (C-band) (Fig 2.b). At 13K, one peak related to the recombination of free excitons known as A-excitons in Wz InP is observed at 1.491 eV.¹⁵ At room temperature, the photoluminescence of InP NWs reveals a peak located at 1.423 eV (the A transition) and a shoulder around 1.458 eV (the B transition). The B transition is observed due to the thermal activation of the holes from the A to the B bands.¹⁵ The

energy splitting between these two bands has been theoretically and experimentally investigated by several groups and values in the 30-50 meV range have been reported.^{15,16,17}

The pressure dependence of the Wz transitions is investigated in the 0-3 GPa range (Figure 3). The position of the A transition could not be determined for pressure higher than 3 GPa because of a weak signal to noise ratio (SNR), due to a decrease of the A peak intensity with pressure. Position of B peak is obtained by the analysis of the 2nd derivative of the spectra.



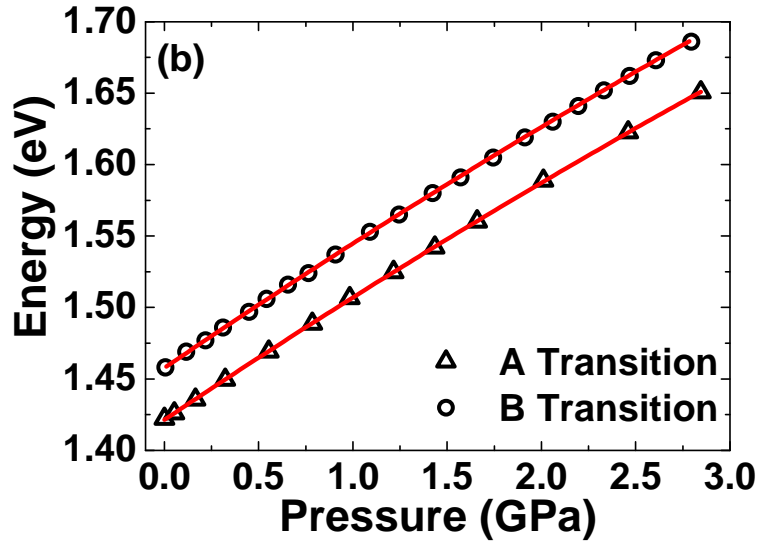


Figure 3: (a) Pressure dependence of PL spectra of InP NWs. (b) Pressure dependence of the A and B transitions. The red lines are the least square fits using Equation (1).

Figure 3.b shows the shift of both A and B transitions as a function of the hydrostatic pressure. The following quadratic equation is used to fit the experimental data:

$$E = E_0 + \alpha P + \beta P^2 \quad (1)$$

which gives linear pressure coefficients of $\alpha_A = 88.2 \pm 0.5$ meV/GPa and $\alpha_B = 89.3 \pm 0.5$ meV/GPa, for A and B transitions, respectively. The value of the quadratic pressure coefficient is the same for both bands: $\beta = -2.7 \pm 0.2$ meV/GPa². The existence of a quadratic pressure coefficient can be explained by nonlinearities in the elastic bulk modulus. In the literature, experimental values in the order of 75 to 84 meV/GPa and in the -1.2 to -1.8 meV/GPa² range have been published for the InP band gap in the ZB crystallographic phase.^{18,19} This means that the linear pressure coefficient of the Wz InP band gap (α_A) is roughly 10% bigger than its value for ZB InP. This observation seems in agreement with theoretical studies on III-Nitride materials.

Comparison of LDA-calculated band-gap pressure coefficients for nitrides in Wz and ZB phases have predicted larger values for the Wz phase.²⁰ The difference between the two crystal phases was in the order of few meV/GPa. This difference could be explained by the extra structural degrees of freedom available in the Wz structure: the variation of the band-gap due to the change in the c/a ratio (where c and a are the hexagonal lattice constants parallel and perpendicular to the [0001] axis), and the internal structural parameter u which represents the relative position of two hexagonal close-packed sublattices.²¹

Theoretical values of α_A and α_B can be calculated from the knowledge of the elastic and potential deformation coefficients. As far as the elastic coefficients are concerned, we use the set calculated using the local density approximation (LDA) by C. Hajlaoui *et al.*²² These coefficients can also be estimated from the ZB ones using a model based on a rotation of the crystal structure and a correction due to the internal strain state (see Table S1 of the supplementary information).^{23,24} For a hydrostatic pressure P , the strain coefficients of a Wz material are:²⁵

$$\varepsilon_{zz} = -\frac{C_{11} + C_{12} - 2C_{13}}{C_{33}(C_{11} + C_{12}) - 2C_{13}^2} P$$

$$\varepsilon_{xx} = \varepsilon_{yy} = \frac{\varepsilon_{\perp}}{2} = -\frac{C_{33} - C_{13}}{C_{33}(C_{11} + C_{12}) - 2C_{13}^2} P \quad (2)$$

Under the assumption of a strain-independent and isotropic spin-orbit interaction, the energies of the A, B and C transitions can be described as:^{26,27}

$$E_A = E_A^0 + (a_{cz} - D_1 - D_3)\varepsilon_{zz} + (a_{ct} - D_2 - D_4)\varepsilon_{\perp} \quad (3)$$

$$E_B = E_B^0 + (a_{cz} - D_1 - \Delta_+ D_3)\varepsilon_{zz} + (a_{ct} - D_2 - \Delta_+ D_4)\varepsilon_{\perp}$$

$$E_C = E_C^0 + (a_{cz} - D_1 - \Delta_- D_3)\varepsilon_{zz} + (a_{ct} - D_2 - \Delta_- D_4)\varepsilon_{\perp}$$

The coefficients Δ_{\pm} are given by:

$$\Delta_{\pm} = \frac{1}{2} \pm \frac{1}{2} \left[1 + 8 \left(\frac{\Delta_3}{\Delta_1 - \Delta_2} \right)^2 \right]^{-1/2} \quad (4)$$

where Δ_1 is the crystal-field splitting and $\Delta_2 = \Delta_3 = \Delta_{SO}/3$ with Δ_{SO} the spin orbit coupling. Here, the experimental values reported in Ref 28, $\Delta_1 = 0.145 \text{ eV}$ and $\Delta_2 = 0.025 \text{ eV}$, are used to obtain the value $\Delta_+ = 0.931$. As far as the deformation potentials of Wz InP material are concerned, sets of parameters have been published in Ref 6 using three different *ab initio* calculation methods: Heyd-Scuseria-Ernzerhof (HSE) density functional theory, generalized-gradient approximation in the Perdew-Burke-Ernzerhof (PBE) parametrization and single shot GW calculations (Table S2 of the supporting information). Another approach is to estimate the deformation potentials in Wz phase from the ZB ones using the quasi-cubic approximation.^{29,30} The extracted theoretical values of the linear pressure coefficients can be found in table I. The elastic coefficients calculated by LDA are used in the PBE, GW and HSE cases. A calculation is also performed using the elastic and deformation potential coefficients obtained from the ZB InP ones using Ref 23 and Ref 29.

	exp results	PBE	GW	HSE	From ZB InP
α_A (meV/GPa)	88.2 ± 0.5	80.3	86.4	88.7	76
α_B (meV/GPa)	89.3 ± 0.5	80.6	86.8	89.0	76
α_C (meV/GPa)		84.9	91	93.4	76

Table I: Experimental results of the present work compared to theoretical calculations of the linear pressure coefficients for the A , B and C bands.

Our experimental results show that the set of parameters obtained by LDA and HSE methods provide a good approximation of the linear coefficients (cf. table I). This study also shows the limits of the quasi cubic approximation for Wz InP. The linear pressure slope calculated from the elastic and deformation potential coefficients of the InP in the ZB phase give values roughly 14% smaller than the measured ones. Moreover A and B bands are assumed to have the same dependence with pressure. This is a consequence of the quasi cubic approximation which implies $\varepsilon_{xx} = \varepsilon_{yy} = \varepsilon_{zz}$ and $D_3 = -2D_4$ which induces a $\alpha_A = \alpha_B$ relation. This experimental study shows that the quasi-cubic approximation, as described in Ref 29, does not provide accurate deformation potentials for the Wz phase and confirms that experimental or theoretical investigations are to be undertaken to have a clear picture of the situation.

A second analysis procedure can be used to extract the effective hydrostatic deformation potentials. The variation of the band gap can be related to the volume change using the relation:⁷

$$E = E_0 + \mathbf{a} \left(1 - \frac{V_0}{V} \right) \quad (5)$$

where \mathbf{a} is the effective hydrostatic deformation potential. The term *effective* is used to highlight the fact that the strain in a Wz structure is not perfectly isotropic under a hydrostatic pressure. The relative volume change caused by the applied pressure can be related to pressure by the Murnaghan equation of state:

$$P = \frac{B}{B'} \left[\left(\frac{V_0}{V} \right)^{B'} - 1 \right] \quad (6)$$

with B the bulk modulus of Wz InP and B' its pressure derivative. The bulk modulus can be calculated using the relation $B = (C_{33}[C_{11} + C_{12}] - 2C_{13}^2) / (C_{11} + C_{12} + 2C_{33} - 4C_{13})$ and a

value of to 69 GPa is calculated. Effective hydrostatic deformation potentials of $\alpha_A = -6.12 \pm 0.04$ eV and $\alpha_B = -6.2 \pm 0.04$ eV are obtained for the A and B transitions, respectively. Moreover the pressure derivatives of the bulk modulus can be deduced from the fit and values of $B'_A = 6.0 \pm 0.4$ and $B'_B = 6.1 \pm 0.4$ are obtained. These values can be compared with the hydrostatic deformation potential of -6.6 eV³¹ and the bulk modulus pressure derivative in the 4-4.6 range for bulk ZB InP.^{32,33} Here again, the Wz phase behavior is quite different from the ZB one, forbidding any approximation of the Wz phase from the ZB one. Contrary to the linear pressure coefficient, the deformation potential is smaller for the Wz phase as compared to the ZB one. This can be explained by the fact that the bulk modulus and its derivative do not have the same values in the Wz and ZB phases.

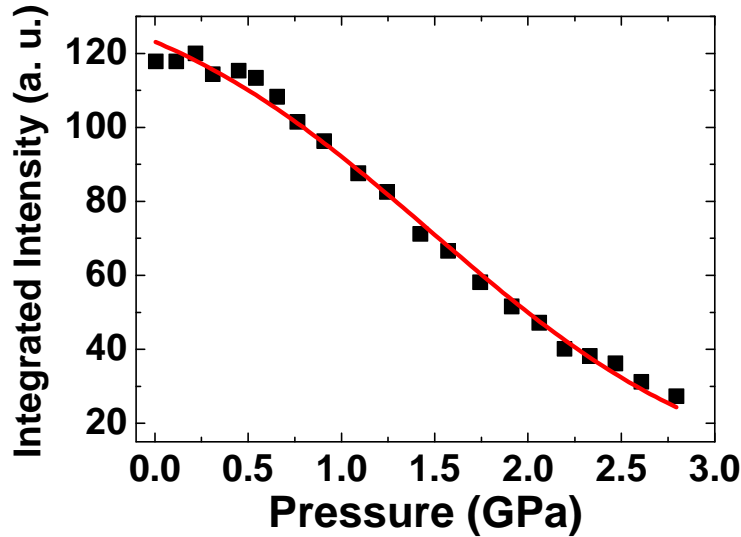


Figure 4: Pressure dependence of the PL integrated intensity.

Figure 4 shows the pressure dependence of the integrated intensity. The PL intensity decreased when the pressure was increased above 0.5 GPa. Such a decrease has already been reported for bulk ZB InP¹⁹ and ZB GaAs³⁴ but for higher pressure (above 6 GPa for InP and 3 GPa for GaAs). In ZB material, this phenomenon is usually explained by the crossing of the Γ and X conduction band minima with increasing pressure and by the transfer of electrons from the Γ to the X valley. The carrier population in the Γ band decreases as $e^{-\Delta E(P)/kT}$ where $\Delta E(P)$ is the energy spacing between the Γ and X minima. The electron transfer from a direct and radiative transition towards an indirect transition induces a strong reduction of the photoluminescence.

The situation is different for the band structure of a wurtzite material. Since the Wz structure has four atoms/cell while the ZB structure has only two atoms/cell, there are twice as many bands per k point in the Wz one. As a consequence the Wz band structure contains two conduction bands: one band having a Γ_7 symmetry and a second band with a Γ_8 symmetry. The second band is related to the states found at the L-point in the ZB phase.^{8,9,4} Electrons with the Γ_7 symmetry can recombine with holes in the A or B bands which induces a strong PL emission due to a direct band gap. On the other hand, for electrons with the Γ_8 symmetry the recombination with holes in the B band is forbidden and the recombination with holes in the A band is called a pseudo-direct transition.

The energy splitting between these two conduction bands is not well known for Wz InP material. Theoretical values of 0.24 eV and 0.4 eV have been reported by Ref 10 and Ref 4, respectively. The experimental probing of the conduction band using highly n-doped Wz InP NWs revealed a value of 0.21 eV,³⁵ while a value of 0.23 eV was reported from photoluminescence excitation (PLE) measurements on undoped NWs.³⁶

We make the assumption that the decrease of the PL emission is related to the transfer of electrons from the Γ_7 to the Γ_8 band. The pressure dependence of the integrated intensity can be described by the equation:

$$I(P) = \frac{I_0}{1 + r e^{-\Delta E(P)/kT}} \quad (7)$$

where $\Delta E(P)$ is the energy spacing between the two conduction bands. A linear equation is used to describe this evolution:

$$\Delta E(P) = \Delta E_0 + \zeta P \quad (8)$$

To fit the experimental results, equation 7 is rewritten as $I(P) = I_0 / (1 + s e^{-\zeta P/kT})$ where I_0 , s and ζ are the fitting parameters. The fitting of the experimental results gives a value $\zeta \approx -0.03 \text{ eV/GPa}$. As the second conduction band in Wz is related to the states found at the L-point in the ZB phase, a rough value of ζ can be estimated from the pressure dependence of the Γ and L bands in ZB InP material. In the case of a hydrostatic deformation, the energy spacing between the Γ and L conduction bands is equal to:

$$E_L^c - E_\Gamma^c = \Delta E_0^c + 3(a_L^c - a_\Gamma^c)\varepsilon$$

$$E_L^c - E_\Gamma^c = \Delta E_0^c - 3 \frac{a_L^c - a_\Gamma^c}{C_{11} + 2C_{12}} P$$

with ΔE_0^c the energy spacing without strain, a_L^c and a_Γ^c the hydrostatic pressure coefficients for the L and Γ valley and C_{11} , C_{12} elastic coefficients of the ZB InP.^{31,20} As a consequence, ζ should be in the order of:

$$\zeta \approx -3 \frac{a_L^c - a_\Gamma^c}{C_{11} + 2C_{12}} \approx -0.04 \text{ eV/GPa}$$

This slope is in the order of magnitude of the experimental value which confirms the hypothesis of an electron transfer from the first to second conduction band. We could also have imagined a redistribution of the holes between the A, B and C valence bands with pressure to explain the decrease of intensity. However, the variation of the energy spacing between the valence bands is in the order of few meV/GPa (Table I) that is one order of magnitude smaller than the experimental value of -30meV/GPa. Thus, hypothesis involving different valence bands can be discarded.

In conclusion, the impact of the pressure has been investigated on Wz InP NWs. The linear and quadratic pressure coefficients have been measured for the A and B transitions. Values equal to $\alpha_A = 88.2 \pm 0.5 \text{ meV/GPa}$, $\alpha_B = 89.3 \pm 0.5 \text{ meV/GPa}$ and $\beta_A = \beta_B = -2.7 \pm 0.2 \text{ meV/GPa}^2$ have been obtained. The linear coefficients are in agreement with ab initio calculations performed in Ref 6 in the HSE DFT framework. The effective hydrostatic deformation potentials have also been extracted for the A and B transitions with values of -6.1 eV and -6.2 eV, respectively. Our results further confirm that approximating the Wz phase behavior from the ZB one is inappropriate. The reduction of the PL intensity upon pressure increase also reveals a reduction of the energy difference between the two conduction band minima at Γ point, leading to a pseudo-direct transition.

ASSOCIATED CONTENT

Supporting Information

TEM investigations of InP NWs, experimental setup and the material parameters used in the analysis. This material is available free of charge via the Internet at <http://pubs.acs.org>.

AUTHOR INFORMATION

Corresponding Author

*E-mail: nicolas.chauvin@insa-lyon.fr.

Funding Sources

This work has been supported by LABEX iMUST (ANR-10-LABX-0064) of Université de Lyon, within the program “Future Investments” (ANR-11-IDEX-0007) operated by the French National Research Agency (ANR) and under the ANR project TEMPOS (reference ANR-10-EQPX-50) obtained in the framework of the "Future Investments" program.

Notes

The authors declare no competing financial interest

ACKNOWLEDGMENT

This work has been supported by LABEX iMUST (ANR-10-LABX-0064) of Université de Lyon, within the program “Investissements d’Avenir” (ANR-11-IDEX-0007) operated by the French National Research Agency (ANR) and by the ANR project TEMPOS (reference ANR-10-EQPX-50) obtained in the framework of the " Future Investments " program. Authors thank P. Regreny, C. Botella, J.B. Goure for technical assistance on the Nanolyon technological platform.

REFERENCES

- (1) Wallentin, J.; Anttu, N.; Asoli, D.; Huffman, M.; Aberg, I.; Magnusson, M. H.; Siefer, G.; Fuss-Kailuweit, P.; Dimroth, F.; Witzigmann, B.; Xu, H. Q.; Samuelson, L.; Deppert, K.; Borgström, M. T. *Science* **2013**, *339*, 1057–1060.
- (2) Wang, Z.; Tian, B.; Paladugu, M.; Pantouvaki, M.; Le Thomas, N.; Merckling, C.; Guo, W.; Dekoster, J.; Van Campenhout, J.; Absil, P.; Van Thourhout, D. *Nano Lett.* **2013**, *13*, 5063–5069.
- (3) Motohisa, J.; Kohashi, Y.; Maeda, S. *Nano Lett.* **2014**, *14*, 3653–3660.
- (4) Bechstedt, F.; Belabbes, A. *J. Phys. Condens. Matter* **2013**, *25*, 273201.
- (5) De, A.; Pryor, C. E. *Phys. Rev. B* **2012**, *85*, 125201.
- (6) Hajlaoui, C.; Pedesseau, L.; Raouafi, F.; Cheikhlarbi, F. Ben; Even, J.; Jancu, J.-M. *J. Phys. D: Appl. Phys.* **2013**, *46*, 505106.
- (7) Shan, W.; Walukiewicz, W.; Ager III, J. W.; Yu, K. M.; Zhang, Y.; Mao, S. S.; Kling, R.; Kirchner, C.; Waag, A. *Appl. Phys. Lett.* **2005**, *86*, 153117.
- (8) Yeh, C.-Y.; Wei, S.-H.; Zunger, A. *Phys. Rev. B* **1994**, *50*, 2715–2718.
- (9) Signorello, G.; Lörtscher, E.; Khomyakov, P. A.; Karg, S.; Dheeraj, D. L.; Gotsmann, B.; Weman, H.; Riel, H. *Nat. Commun.* **2014**, *5*, 3655.
- (10) De, A.; Pryor, C. E. *Phys. Rev. B* **2010**, *81*, 155210.
- (11) Naji, K.; Saint-Girons, G.; Penuelas, J.; Patriarche, G.; Largeau, L.; Dumont, H.; Rojo-Romeo, P.; Gendry, M. *Appl. Phys. Lett.* **2013**, *102*, 243113.
- (12) Chauvin, N.; Hadj Alouane, M. H.; Anufriev, R.; Khmissi, H.; Naji, K.; Patriarche, G.; Bru-Chevallier, C.; Gendry, M. *Appl. Phys. Lett.* **2012**, *100*, 011906.
- (13) Yu, H.; Li, J.; Loomis, R. A.; Wang, L.-W.; Buhro, W. E. *Nat. Mater.* **2003**, *2*, 517–520.
- (14) Dos Santos, C. L.; Piquini, P. *Phys. Rev. B* **2010**, *81*, 075408.
- (15) Zilli, A.; Luca, M. De; Tedeschi, D.; Fonseka, H. A.; Miriametro, A.; Tan, H. H.; Jagadish, C.; Capizzi, M.; Polimeni, A. *ACS Nano* **2015**, *9*, 4277–4287.
- (16) Gadret, E.; Dias, G. O.; Dacal, L. C. O.; de Lima Jr., M. M.; Ruffo, C. V. R. S.; Iikawa, F.; Brasil, M. J. S. P.; Chiaramonte, T.; Cotta, M. A.; Tizei, L. H. G.; Ugarte, D.; Cantarero, A. *Phys. Rev. B* **2010**, *82*, 125327–5.
- (17) Perera, S.; Pemasiri, K.; Fickenscher, M. A.; Jackson, H. E.; Smith, L. M.; Yarrison-Rice, J.; Paiman, S.; Gao, Q.; Tan, H. H.; Jagadish, C. *Appl. Phys. Lett.* **2010**, *97*, 023106–3.
- (18) Muller, H.; Trommer, R.; Cardona, M.; Vogl, P. *Phys. Rev. B* **1980**, *21*, 4879–4883.
- (19) Menoni, C. S.; Hochheimer, H. D.; Spain, I. L. *Phys. Rev. B* **1986**, *33*, 5896–5898.
- (20) Wei, S.-H.; Zunger, A. *Phys. Rev. B* **1999**, *60*, 5404–5411.
- (21) Christensen, N. E.; Gorczyca, I. *Phys. Rev. B* **1994**, *50*, 4397–4415.

- (22) Hajlaoui, C. PhD Thesis, INSA Rennes, El Manar Tunis University, 2014.
- (23) Martin, R. M. *Phys. Rev. B* **1972**, *6*, 4546–4553.
- (24) Larsson, M. W.; Wagner, J. B.; Wallin, M.; Håkansson, P.; Fröberg, L. E.; Samuelson, L.; Wallenberg, L. R. *Nanotechnology* **2007**, *18*, 015504.
- (25) Peng, H. Y.; McCluskey, M. D.; Gupta, Y. M.; Kneissl, M.; Johnson, N. M. *Phys. Rev. B* **2005**, *71*, 115207.
- (26) Gil, B.; Briot, O.; Aulombard, R.-L. *Phys. Rev. B* **1995**, *52*, R17028.
- (27) Shan, W.; Hauenstein, R. J.; Fischer, A. J.; Song, J. J.; Perry, W. G.; Bremser, M. D.; Davis, R. F.; Goldenberg, B. *Phys. Rev. B* **1996**, *54*, 13460–13463.
- (28) Hadj Alouane, M. H.; Chauvin, N.; Khmissi, H.; Naji, K.; Ilahi, B.; Maaref, H.; Patriarche, G.; Gendry, M.; Bru-Chevallier, C. *Nanotechnology* **2013**, *24*, 035704.
- (29) Sirenko, Y. M.; Jeon, J. B.; Lee, B. C.; Kim, K. W.; Littlejohn, M. A.; Stroschio, M. A.; Iafate, G. J. *Phys. Rev. B* **1997**, *55*, 4360–4375.
- (30) Faria Junior, P. E.; Sipahi, G. M. *J. Appl. Phys.* **2012**, *112*, 103716.
- (31) Vurgaftman, I.; Meyer, J. R.; Ram-Mohan, L. R. *J. Appl. Phys.* **2001**, *89*, 5815–5875.
- (32) Soma, T.; Takahashi, Y.; Kagaya, H.-M. *Solid State Commun.* **1985**, *53*, 801–803.
- (33) Menoni, C. S.; Spain, I. L. *Phys. Rev. B* **1987**, *35*, 7520–7525.
- (34) Yu, P. Y.; Welber, B. *Solid State Commun.* **1978**, *25*, 209–211.
- (35) Wallentin, J.; Mergenthaler, K.; Ek, M.; Wallenberg, L. R.; Samuelson, L.; Deppert, K.; Pistol, M.-E.; Borgstrom, M. T. *Nano Lett.* **2011**, *11*, 2286–2290.
- (36) Perera, S.; Shi, T.; Fickenscher, M. A.; Jackson, H. E.; Smith, L. M.; Yarrison-Rice, J. M.; Paiman, S.; Gao, Q.; Tan, H. H.; Jagadish, C. *Nano Lett.* **2013**, *13*, 5367–5372.